



# Method operable design region obtained with a partial least squares model inversion in the determination of ten polycyclic aromatic hydrocarbons by liquid chromatography with fluorescence detection



M.M. Arce<sup>a</sup>, S. Sanllorente<sup>a</sup>, S. Ruiz<sup>b</sup>, M.S. Sánchez<sup>b</sup>, L.A. Sarabia<sup>b</sup>, M.C. Ortiz<sup>a,\*</sup>

<sup>a</sup> Dep. Química, Universidad de Burgos, Facultad de Ciencias, Plaza Misael Bañuelos s/n, 09001 Burgos, Spain

<sup>b</sup> Dep. Matemáticas y Computación, Universidad de Burgos, Facultad de Ciencias, Plaza Misael Bañuelos s/n, 09001 Burgos, Spain

## ARTICLE INFO

### Article history:

Received 27 July 2021

Revised 17 September 2021

Accepted 18 September 2021

Available online 24 September 2021

### Keywords:

Method operable design region

Analytical quality by design

PLS model inversion

Polycyclic aromatic hydrocarbon

HPLC-FLD

Pareto front

## ABSTRACT

A chromatographic method with the Analytical Quality by Design (AQbD) methodology is developed for the simultaneous determination by HPLC-FLD of ten PAHs (naphthalene, phenanthrene, anthracene, fluoranthene, pyrene, chrysene, benzo[a]anthracene, perylene, benzo[b]fluoranthene, and benzo[a]pyrene), widely spread in the environment.

The construction of the Method Operable Design Region (MODR) is conducted, for the first time, via the inversion of a multiresponse Partial Least Squares (PLS2) model, which is needed to maintain the correlations among the Critical Method Parameters (CMP), among the Critical Quality Attributes (CQA), and the covariance between one another.

The five CMP considered were the composition of the mobile phase (water, methanol, acetonitrile), flow rate, and column temperature. The eight CQA were linked to resolution between peaks recorded in the same emission wavelength (greater than 1.4) and the total time (less than 15 minutes).

By systematic use of experimental design and parallel coordinates plots to explore the Pareto optimal front obtained with the PLS2 model inversion, the computed MODR is formed by convex combinations of eight specific settings of Critical Method Parameters that have a mobile phase with percentages of water between 37 and 38 %, of methanol from 13 and 22 %, and of acetonitrile between 41 and 49 %, together with a flow rate between 1.47 and 1.50 mL min<sup>-1</sup>, and column temperature between 41.9 and 44.0 °C in their adequate combinations.

All the chromatographic peaks are well resolved, with total time varying between 12.96 and 15.66 min inside the estimated MODR and the analytical method is accurate with CC $\beta$  between 0.9 and 7.0  $\mu$ g L<sup>-1</sup> with probability of both false positive and false negative equal to 0.05.

© 2021 The Author(s). Published by Elsevier B.V.

This is an open access article under the CC BY-NC-ND license (<http://creativecommons.org/licenses/by-nc-nd/4.0/>)

## 1. Introduction

The concept of Quality by Design (QbD) was introduced in 2004 by the U.S. Food and Drug Administration (FDA) [1] and approved in 2005 by the International Council for Harmonisation of Technical Requirements for Pharmaceuticals for Human Use (ICH) [2]. Since analytical procedures are also processes inside the global pharmaceutical-product process [3], the application of QbD to the development of analytical methods is called Analytical Quality by Design (AQbD).

The first step in AQbD is the definition of the intended purpose of the analytical method throughout the so-called Analytical Target Profile (ATP). The ATP contains the criteria defining what will be measured, in which matrix, over what concentration range, and the required performance criteria of the method, together with specifications for the latter [3]. To maintain a nomenclature close to that used in the pharmaceutical field, these performance criteria are usually called Critical Quality Attributes (CQA) of the analytical method, and depend upon the Critical Method Parameters (CMP).

The relation between CMP and CQA is described with a mathematical prediction model, which is used to define the Method Operable Design Region (MODR). The MODR is a region inside the allowed limits of variation of CMP where the preset ATP is fulfilled, so that the analytical method is robust in that region. In

\* Corresponding author.

E-mail address: [mcortiz@ubu.es](mailto:mcortiz@ubu.es) (M.C. Ortiz).

other words, the MODR can provide suitable method performance. A theoretical background with a workflow of AQbD, and some applications can be found in Refs. [4–7].

Inside AQbD, the Design of Experiments (DOE) is a key element to construct the relation (model) between CMP and CQA, which should be multivariate, multiresponse and highly predictive. However, methodologically and conceptually, AQbD is a much broader scenario. Back in 2015 [7] and later in 2021 [4], Peraman *et al.* already stated that several authors erroneously believe that AQbD is just to optimize an analytical method by using DOE and omitting the need of obtaining the MODR after defining the desired values of CQA. Their assertion seems to be accurate because a search in the Scopus database (2010–2020) with “Analytical Quality by Design OR AQbD” in title, abstract, or keywords returns 143 papers, whereas the search “Method Operable Design Region OR MODR OR design space” returns 53 papers in the same time period, that is, only 37 % of the applications of AQbD explicitly consider the construction of the MODR.

As the MODR is the ‘core’ of AQbD, its computation is essential to guarantee the required specifications in CQA. There are several approaches to compute the MODR [3] including Monte Carlo simulations, or bootstrap or Bayesian techniques [8]. Also, a widely used strategy to define the MODR is by using contour plots of the fitted responses and then performing Monte Carlo simulations [5].

Response Surface Methodology is related to the practice of fitting the mathematical relation between CMP and CQA by response surfaces, separately for each different specification defined in the ATP. Thus, each of the CQA acts in turn as a single response in an experimental domain. The effects of CMP are then visualized by drawing contour plots of the response surfaces for each property or specification. Since frequently there is more than one CQA, it is usual to overlap the different plots to handle the global optimization so that the plots are used to identify the areas where the predicted values of CQA fulfill the individual specifications.

Another consideration when fitting individual quadratic models (response surfaces) for each CQA specification is that this approach, usual in the literature, does not take into account the correlation among these specifications, which is expected to be high. Additional advantages of using regression methods based on latent variables, instead of individual response surfaces, include that they discard the variation of the CMP which is not related to the variation observed in the CQA (in other words, all the domain where the CMP can vary would not be needed to explain the variation of the CQA). Nevertheless, latent variable models are rarely utilized, except for the use of a Partial Least Squares (PLS) model in Ref. [9] or the PLS2 models used in Refs. [10,11] to simultaneously predict all the CQA.

The present work tackles, for the first time, the determination of a MODR when the relation CMP/CQA is built by means of a PLS2 regression model. In brief, the inversion of the fitted PLS2 model, as presented in Ref. [12], provides the CMP to obtain the Pareto front for the CQA, which means the CMP needed to obtain optimal values in at least one of the specifications set in the ATP. The analysis of these CMP allows selecting those that belong to the MODR, which can be then defined with their convex envelope.

Although the study is posed in the context of how industry is concerned with QbD issues, the proposed methodology may be of wider utility, not only for estimating the MODR, but also as a way to minimize how many “possible” experiments need to be conducted to achieve the intended performance of the analytical method applied.

The strategy is followed for the determination of a subset of the experimental domain where the chromatographic factors in an HPLC-FLD procedure can be varied without distorting the quality of the chromatograms needed to determine ten polycyclic aromatic hydrocarbons (PAHs). The aim set in the ATP includes adequate

separation of the ten analytes and to reduce the time for obtaining the chromatogram (saving time and solvents). Consequently, the CQA defined for this work are the resolutions between contiguous peaks for each emission wavelength recorded and the final time. All the computed solutions inside the MODR are experimentally validated for the intended determination.

Polycyclic aromatic hydrocarbons are a group with more than a hundred different organic compounds, which are generated in the environment, mainly during the incomplete combustion of organic matter [13]. Among the hundreds of known PAHs, 16 have been designated as high priority pollutants by the United States Environmental Protection Agency (EPA) [14].

The concern about these 16 PAHs is due to their potential toxicity to humans and other organisms and because of their prevalence and persistence in the environment. In addition, the 16 PAHs appear on the International Agency for Research on Cancer (IARC) list in some of the four categories, with benzo[a]pyrene (BaP) included in group 1 “carcinogenic to humans” [15].

Polycyclic aromatic hydrocarbons are part of the foodstuff regulated in Europe via Commission Regulation (EC) No 1881/2006 setting maximum levels for certain contaminants in foodstuffs [16]. Commission Regulation (EU) No 835/2011 of 19 August 2011 amending Regulation (EC) No 1881/2006 sets maximum levels for polycyclic aromatic hydrocarbons in foodstuffs [17]. This modification takes into account the conclusions drawn by the European Food Safety Authority (EFSA) about the inadequacy of using the quantity of BaP as unique marker of the total content of PAHs and introduces a new marker for the maximum allowable level, which is the sum of the content of four compounds (PAH4): BaP, benzo[a]anthracene (BaA), benzo[b]fluoranthene (BbF) and chrysene (CHR), in addition to maintaining a maximum content of BaP.

Ten polycyclic hydrocarbons have been selected in this study to apply the proposed methodology: perylene and another nine included in the EPA list, namely naphthalene, phenanthrene, anthracene, fluoranthene, pyrene, chrysene, benzo[a]anthracene, benzo[b]fluoranthene, and benzo[a]pyrene.

## 2. Material and methods

### 2.1. Chemicals and reagents

Naphthalene (NAP 99 %, CAS no. 91-20-3), anthracene (ANT  $\geq$  98 %, CAS no. 120-12-7), fluoranthene (FLN  $\geq$  98 %, CAS no. 206-44-0), perylene (PER  $\geq$  99 %, CAS no. 198-55-0) and benzo[b]fluoranthene (BbF 98 %, CAS no. 205-99-2) were acquired in Sigma-Aldrich (Steinheim, Germany). Phenanthrene (PHE 98 %, CAS no. 85-01-8), pyrene (PYR 98 %, CAS no. 129-00-0) and benzo[a]pyrene (BaP 96 %, CAS no. 50-32-8) were purchased by Alfa Aesar (Kandel, Germany). Benzo[a]anthracene (BaA 99 %, CAS no. 56-55-3) was bought from Acros Organic (Geel, Belgium). Chrysene (CHR  $\geq$  95 %, CAS no. 218-01-9), acetonitrile (CAS no. 75-05-8; LiChrosolv® isocratic grade for liquid chromatography) and methanol (CAS no. 67-56-1; LiChrosolv® isocratic grade for liquid chromatography) were supplied by Merck (Darmstadt, Germany). Deionized water was obtained by using the Milli-Q gradient A10 water purification system from Millipore (Bedford, MA, USA).

### 2.2. Instrumental

The determination of the ten polycyclic aromatic hydrocarbons, NAP, PHE, ANT, FLN, PYR, CHR, BaA, PER, BbF, and BaP, was carried out by using an Agilent 1260 Infinity HPLC chromatograph (Santa Clara, CA, USA) consisting of a quaternary pump (G1311C), a sampler (G1329B), a thermostatic column compartment (G1316A), and a fluorescence detector (G1321B). A Kinetex EVO-C18 column

(150 mm × 4.6 mm, 5 μm) was used for the separation. Deionized water, methanol, and acetonitrile were used as mobile phases.

The conditions for chromatographic analyses were programmed in isocratic elution mode. Mobile phase consists of different percentages of a mixture of water/methanol/acetonitrile ( $Z_1:Z_2:Z_3$ , v/v) with different mobile phase flow rate ( $X_4$ , mL min<sup>-1</sup>) and column temperature ( $X_5$ , °C), depending on the conditions in the different experiments conducted, which are explained in the following sections (3.1, 3.3 and 3.4).

In all analyses, the injection volume was 10 μL. Fluorescence detector was programmed to measure the fluorescence intensity at a fixed excitation wavelength of 274 nm. However, three emission wavelengths were selected to better identification of the ten PAHs in chromatograms, being 345 nm the one for NAP and PHE, 405 nm for ANT, PYR, CHR, BaA, and BaP, and 470 nm for FLN, PER, and BbF.

For each wavelength, the resolution  $Rs_{i,i+1}$  between the consecutive  $i$ -th and  $(i+1)$ -th chromatographic peaks is calculated with Eq. 1, where  $t_{R,i}$  is the retention time and  $w_{0.5,i}$  is the width at half height of the  $i$ -th chromatographic peak.

$$Rs_{i,i+1} = \frac{2.35(t_{R,i+1} - t_{R,i})}{2(w_{0.5,i+1} + w_{0.5,i})} \quad (1)$$

As an example, Fig. 1 shows the results with three experimental conditions (three chromatograms recorded per injection). The run in Fig. 1A) takes too long (180 minutes), the one in Fig. 1B), although the chromatogram takes less time, shows a severe overlapping between contiguous peaks in the three wavelengths, and Fig. 1C) shows one experiment that belongs to the Method Operable Design Region obtained in section 3.4, with no overlapping peaks. Fig. 1 caption contains the details about the used experimental conditions.

### 2.3. Standard solutions and samples

Individual standard stock solutions of 100 mg L<sup>-1</sup> were prepared by dissolving each standard in acetonitrile and stored frozen and protected from light. Intermediate solutions of 10 mg L<sup>-1</sup> of each PAH were prepared from the individual stock solutions by dilution with acetonitrile. With the aim of recording similar signal intensities for the ten PAHs, a mixture with different concentration levels of each PAH was prepared from the intermediate solutions by dilution with acetonitrile. These concentration levels were 500, 500, 2000, 300, 150, 100, 40, 200, 150, and 30 μg L<sup>-1</sup> for NAP, PHE, ANT, FLN, PYR, CHR, BaA, PER, BbF, BaP, respectively.

This mixture solution was used for the experiments carried out according to a D-optimal design explained in section 3.1. Because a month had last since D-optimal experiments were carried out, new intermediate solutions and mixture solution were prepared for the experimental exploration of the MODR in sections 3.3 and 3.4.

For fitting calibration and accuracy lines and computing the capability of detection in section 3.5, apart from the mixture solution previously named, ten additional ones (with crossed concentration levels for each PAH) were prepared from the intermediate solutions by dilution with acetonitrile. All the solutions were stored protected from light at 4 °C.

### 2.4. Software

OpenLab CDS ChemStation software was used for acquiring data. The PLS2 models were fitted with the PLS\_Toolbox [18] for use with MATLAB™ [19]. The inversion of the PLS2 model and the Pareto front were computed with in-house programs written in MATLAB™ code. The D-optimal experimental design is selected with NEMRODW [20].

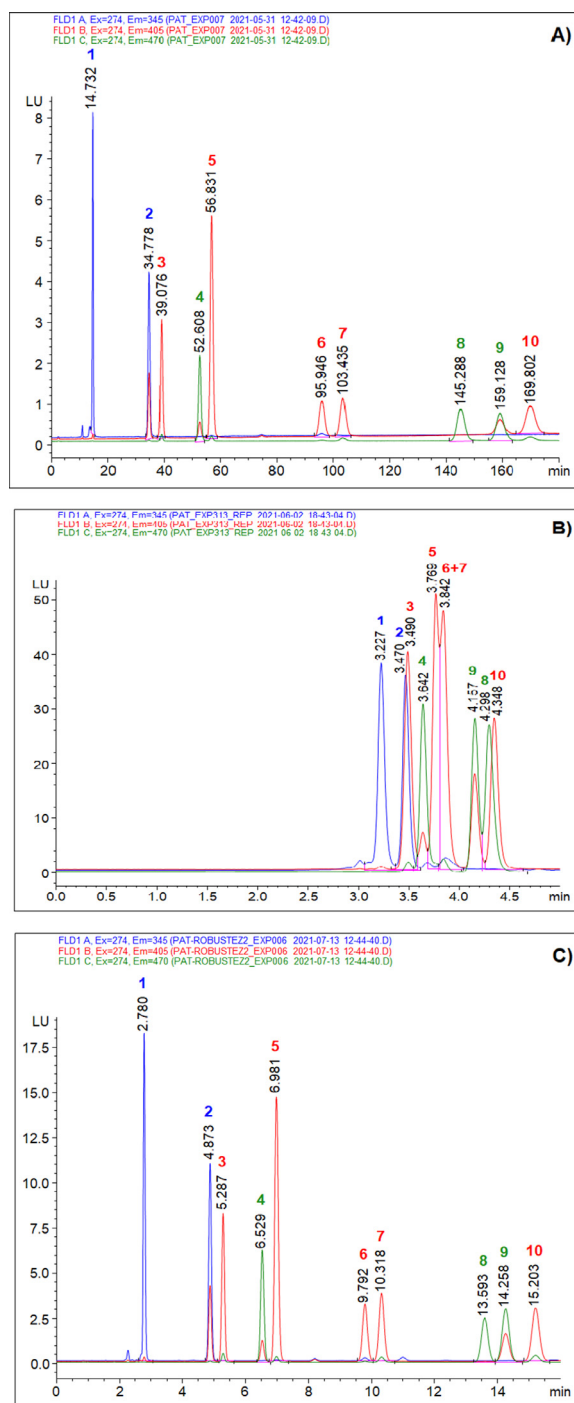


Fig. 1. Chromatograms recorded at three emission wavelengths (345 nm in blue, 405 nm in red, and 470 nm in green) for three different compositions and flow rate of the mobile phase, and column temperature: A) 40:60:0 (water/methanol/acetonitrile), 0.5 mL min<sup>-1</sup>, and 44 °C; B) 0:100:0, 0.5 mL min<sup>-1</sup>, and 44 °C; and C) 38:19:43, 1.5 mL min<sup>-1</sup>, and 42 °C. Peak identification: 1) NAP, 2) PHE, 3) ANT, 4) FLN, 5) PYR, 6) CHR, 7) BaA, 8) PER, 9) BbF and 10) BaP.

## 3. Results and discussion

The proposed procedure, described below, is general and can be used with other problems in AQbD. However, in the following sections it will be applied to obtain the MODR in the specific case of the determination of ten PAHs by HPLC-FLD.

The estimation of the Method Operable Design Region in the framework of AQbD is developed through PLS2 model inversion,

that requires a proper PLS2 prediction model fitted to relate the settings of  $p$  CMP in matrix  $\mathbf{X} = (X_1, X_2, \dots, X_p)$  to  $\mathbf{Y} = (Y_1, Y_2, \dots, Y_m)$  with the values of  $m$  CQA, that is,  $m$  experimental responses.

The procedure consists of four steps:

- Step 1. To select a set of experimental conditions adequate to cover the feasible domain of the Critical Method Parameters. To do it, an experimental design is used with an affordable number of experiments and related to the proposed relation between CMP and CQA. The resulting chromatograms obtained with the experimental conditions in the design are characterized in terms of the CQA, which in turn helps in deciding the proper specifications for them.
- Step 2. To build a single (vector) mathematical model,  $\mathbf{Y} = f(\mathbf{X})$ , by partial least squares (PLS2 model), not only to describe the CQA as a function of the CMP but also to consider the correlation structure among the experimental values of the CQA in  $\mathbf{Y}$  and among the values of CMP in  $\mathbf{X}$ . The computational inversion of this model towards getting the Pareto front with the conditions imposed to the CQA (in the present work, improve resolutions and reduce time), provides experimental conditions with which at least one of the expected values of the CQA is optimum. The analysis of the obtained settings for the CMP and their expected CQA values in the Pareto front shows the extension of the conflict among the responses (values of CQA) and the range of the values that can be achieved, therefore evaluating the possibility of reaching the specifications proposed in the ATP. If this is the case, the Pareto optimal solutions that comply with the CQA limits serve themselves as an initial estimation of the MODR.
- Step 3. To experimentally validate the MODR obtained in step 2 in the form of a discrete domain, which is analyzed to choose some representative experimental conditions. The experiments conducted with them provide chromatograms whose characteristics serve to evaluate the compliance of the CQA. If necessary, the MODR is reduced to the convex envelope of the CMP that provided compliant chromatograms. This step is required because the PLS2 model, like any other least squares based regression model, is good in predicting mean values but not necessarily every individual value. Therefore, the estimated MODR is a discrete set with  $n$  chromatographic conditions:

$$\text{MODR} = \{\mathbf{X}_i = (x_{i1}, x_{i2}, \dots, x_{ip}), i = 1, \dots, n\} \quad (2)$$

- Step 4. It is an optimal step if the MODR is to be defined as a 'geometrical' region. To maintain the correlation among CMP, only convex combinations of the  $n$  elements in the MODR are used, that is, the values obtained as  $\lambda\mathbf{X}_i + (1 - \lambda)\mathbf{X}_j$  for  $\mathbf{X}_i, \mathbf{X}_j \in \text{MODR}$  in Eq. 2 and  $0 \leq \lambda \leq 1$ . These convex combinations give new CMP values that should be also experimentally validated.

### 3.1. Experimental design

A thorough bibliographical revision (summarized in Table S1 of the supplementary material and discussed in section 3.5) led to the selection of five Critical Methods Parameters (the ternary composition and flow rate of the mobile phase, and the column temperature), that can be varied and whose variation changes the resulting chromatogram, as can be seen in Fig. 1.

The first three CMP specify the proportion of water ( $Z_1$ ), methanol ( $Z_2$ ), and acetonitrile ( $Z_3$ ) in the composition of the mobile phase. The acetonitrile of water in the mixture should be less than 40 % with no restriction in the composition of methanol and

acetonitrile. The particular proportions to conduct the experiments are selected following a mixture design in a restricted simplex.

The fourth and fifth factors, flow rate of the mobile phase and column temperature, are continuous factors that vary between 0.5 and 1.5 mL min<sup>-1</sup>, and from 20 to 44 °C, respectively. Table 1 summarizes the stated conditions that define the experimental domain. From a DOE point of view,  $Z_1, Z_2$ , and  $Z_3$  constitute the components of a mixture (varying on a restricted simplex), and factors  $X_4$  and  $X_5$  are continuous factors.

To obtain a 'representative' training set that adequately covers the experimental domain, the experiments conducted followed an experimental design. As there are proportions of a mixture and two continuous factors, the design is a combined design (with mixture and process variables) in the domain defined in Table 1. The experimental design began with 405 candidate points (45 of the mixture design, 3 levels for the flow rate, and another 3 levels for column temperature). With a multiplicative mixture process model, quadratic in the continuous variables (flow rate and temperature), the algorithm to compute the D-optimal design [20] provides 42 experiments with the maximum of the variance function [21] equal to 0.91, including 16 protected experimental points. These protected points correspond to four ternary mixtures selected from a uniform grid (width 0.1) in the restricted simplex in the high and low levels of both mobile phase flow rate and column temperature.

Lastly, after a selection of predictor variables, the final model for each individual response in the multiplicative mixture process design is linear in the continuous variables (flow rate and column temperature), with a quadratic dependence on the mixture composition ( $Z_1, Z_2, Z_3$ ).

### 3.2. Fitting and inversion of a prediction model

Therefore, there are five experimental factors (the CMP), namely the ternary mixture and flow rate of the mobile phase, and column temperature. The Critical Quality Attributes (CQA) are defined in terms of the resolution between contiguous chromatographic peaks (for the three emission wavelengths used to record the chromatograms) as well as the final time needed to finish the chromatograms. Consequently, there is a total of eight characteristics (eight CQA) to be measured for each experiment.

However, interactions and/or strong nonlinear effects of the factors on the responses are expected. The model fitted, in Eq. 3, considers them through its 27 coefficients ( $\beta$ 's) that account up to interactions between components of the mixture ( $Z_i$ ) and process variables ( $X_j$ ).

$$\begin{aligned} \mathbf{Y} = & \beta_1 Z_1 + \beta_2 Z_2 + \beta_3 Z_3 + \beta_4 X_4 + \beta_5 X_5 + \beta_{12} Z_1 Z_2 \\ & + \beta_{13} Z_1 Z_3 + \beta_{23} Z_2 Z_3 + \sum_{j=1}^3 (\beta_{4j} X_4 Z_j + \beta_{5j} X_5 Z_j) + \beta_{45} X_4 X_5 \\ & + \sum_{j=4}^5 (\beta_{12j} Z_1 Z_2 X_j + \beta_{13j} Z_1 Z_3 X_j + \beta_{23j} Z_2 Z_3 X_j) + \sum_{j=1}^3 \beta_{45j} X_4 X_5 Z_j \\ & + \beta_{1245} Z_1 Z_2 X_4 X_5 + \beta_{1345} Z_1 Z_3 X_4 X_5 + \beta_{2345} Z_2 Z_3 X_4 X_5 \end{aligned} \quad (3)$$

where  $\mathbf{Y}$  denotes the matrix of responses, with eight columns, first the resolutions, then the final time.

As there is more than one response, a PLS2 model was fitted. The final time had to be logarithmically transformed (decimal logarithm) for the fitting. Nevertheless, in the following, when speaking about the final time, the transformation will be undone to better illustrate the discussion.

Therefore, matrix  $\mathbf{X}$  of predictor variables is 45 x 27 (45 experiments, 42 from the D-optimal design plus 3 replicates), and matrix  $\mathbf{Y}$  with the responses is 45 x 8. In particular, responses  $Y_1, \dots, Y_7$  refers to the resolution ( $R_s$ ) between peaks identified by the

**Table 1**  
CMP (experimental factors) and their variation.

Factor	Lower bound	Upper bound	Centre	Step of variation
Z <sub>1</sub> Water	0.000	0.400		
Z <sub>2</sub> Methanol	0.000	1.000		
Z <sub>3</sub> Acetonitrile	0.000	1.000		
X <sub>4</sub> Flow rate (mL min <sup>-1</sup> )			1.000	0.500
X <sub>5</sub> Temperature (°C)			32.0	12.0

**Table 2**  
Coefficients of determination, R<sup>2</sup>, for each individual response Y<sub>i</sub> and their estimations in prediction, computed by crossvalidation, R<sub>cv</sub><sup>2</sup>.

	Y <sub>1</sub>	Y <sub>2</sub>	Y <sub>3</sub>	Y <sub>4</sub>	Y <sub>5</sub>	Y <sub>6</sub>	Y <sub>7</sub>	Y <sub>8</sub>
R <sup>2</sup>	0.9867	0.9824	0.9877	0.9749	0.9777	0.9861	0.9701	0.9889
R <sub>cv</sub> <sup>2</sup>	0.9538	0.9457	0.9609	0.9345	0.9431	0.9604	0.9127	0.9599

same emission wavelength, computed as in Eq. 1 with the peak identification in Fig. 1, Y<sub>1</sub> = Rs<sub>12</sub>, Y<sub>2</sub> = Rs<sub>35</sub>, Y<sub>3</sub> = Rs<sub>56</sub>, Y<sub>4</sub> = Rs<sub>67</sub>, Y<sub>5</sub> = Rs<sub>710</sub>, Y<sub>6</sub> = Rs<sub>48</sub> and Y<sub>7</sub> = Rs<sub>89</sub>, and log<sub>10</sub>(t<sub>f</sub>), which is Y<sub>8</sub>.

With autoscaled predictor and responses variables, and cross-validation with venetian blinds (five splits and blind thickness equal to one), a model with 11 latent variables was selected, that explains 97.93 % of the variance in **X** with 98.18 % in **Y**. The coefficient of determination for every individual response in both fitting and crossvalidation is in Table 2. The similarity of the explained variance in fitting and prediction points to highly predictive models. The worst value is 0.9127 for the prediction estimation (computed by crossvalidation) with response Y<sub>7</sub> (resolution between PER and BbF). Also a permutation test to evaluate over-fitting has been made and the probability that the PLS2 model is significantly different from another one built under the same conditions but on random data is always less than 0.005 in fitting and in prediction. The conclusion is that the fitted PLS2 model adequately predicts all eight responses.

Therefore, the PLS2 model will be used to predict the expected characteristics of the chromatograms obtained with different experimental conditions in the experimental domain defined by the five CMP. Nevertheless, the usual situation is to know the sought characteristics and need to find the experimental conditions, if any, to obtain them. This 'reverse' situation is referred to as inversion of the model, more precisely in the present case, as latent variable model inversion [22] (see the introduction in Ref. [23] for an up-to-date description and Refs. [12,24] for further information).

As already said in the introduction, the desired characteristics for the chromatograms when jointly determining the ten PAHs are defined in the ATP. For the present case, it requires that every resolution is greater than 1.4 and that the final time is as short as possible, but not greater than 15 minutes.

The inversion of the model should provide the experimental conditions (five-dimensional vector with the CMP) for obtaining characteristics of the chromatograms close to the specification for the CQA (eight-dimensional vector), which makes the algebraic inversion undetermined. It is in fact undefined [24] because the PLS2 model is fitted with 27 variables, not with the 5 needed. Therefore, for obtaining experimental conditions that give chromatograms with characteristics close to those defined in the ATP, the computational alternative explained in Ref. [12] was used.

In a multiobjective or multiresponse optimization situation, the procedure for the inversion looks for the input variables that define the Critical Method Parameters (CMP) which predict the CQA by using a prediction model, subject to several constraints to remove unfeasible or unpractical solutions.

Since no information is available on the possible conflicting behavior among resolutions and with the final time, nor about the extent of said conflict, an exploration run was carried out. This

goal (the exploration) is different from just the optimization of a chromatographic separation that can consider other optimization criteria [25], like the critical resolution instead of all resolutions.

Therefore, the multiobjective function to be optimized will be the vector function whose components are the predicted responses, i.e., a vector ( $\hat{y}_1, \hat{y}_2, \dots, \hat{y}_8$ ) for a given setting of CMP. The goal is to obtain a good peak resolution in the first seven coordinates, and to minimize the decimal logarithm of the final time, which is a monotonically increasing function, thus, the final time is also minimized.

The optimization engine is an evolutionary algorithm that provides the optimal solutions among those that belong both to the domain and the so-called PLSbox [24], that is, the region defined by the 95 % confidence levels of Q and T<sup>2</sup> statistics, established when building the PLS prediction model.

Starting with an initial population of points complying with the above-mentioned constraints, the usual genetic operators (selection, crossover, and mutation) are used to create new potential solutions and updating the population in each generation to move towards the Pareto optimal front, or simply Pareto front. In this multiobjective optimization setting, the Pareto front contains the set of values that are the best in at least one of the responses under study in such a way that it is impossible to move along the Pareto front trying to gain in one response without losing something in another.

The high correlation among responses and between the experimental conditions and the resulting characteristics of the chromatograms (resolution and time) make this approach appealing because the Pareto front will describe the extent of the conflict resulting from these high correlations, providing different solutions (different chromatograms obtained with different experimental conditions) that can be considered 'equivalent' for the determination of the ten PAHs. In other words, a discrete estimation of a region of model robustness (inside the MODR) or a subset of the so-called design space [2].

For 100 times with population size of 150 and probability of mutation equal to 0.1 evolving for 700 generations, a total of 1727 solutions are part of the Pareto front. The conflict among responses results in solutions with large resolution that will take excessive time, or short runs with very poor resolution among peaks. The Pareto front also shows that the resolutions likely to be lost when decreasing the final time are only two, Rs<sub>67</sub> (Y<sub>4</sub>) and Rs<sub>89</sub> (Y<sub>7</sub>), specially the latter. In any case, there are several settings of the CMP with which their predictions are greater than 1.4.

Therefore, the first selection inside the Pareto front is made by only retaining solutions with all the peak resolutions greater than or equal to 1.5 and total time less than 14 minutes. As can be observed, the threshold values imposed are 'conservative' with respect to the set ATP specifications, just as a first precaution

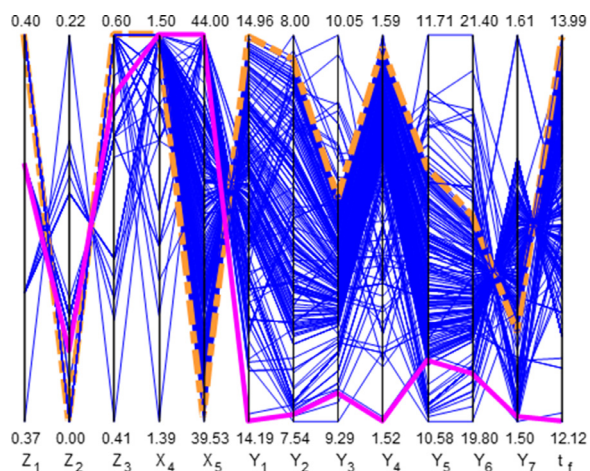


**Fig. 2.** Parallel Coordinates Plot of the Pareto optimal solutions with all resolutions at least 1.5 and final time less than 14 minutes. The colors highlight different behaviors.

and also because the results of the exploration run show that the achievable ranges allow these additional restrictions. The retained 300 solutions thus contain the experimental conditions that are expected to provide chromatograms which comply with the specified limits for CQA.

Fig. 2 is the parallel coordinates plot of these 300 results, the first five coordinates contain the experimental factors (proportion of water, methanol, and acetonitrile, flow rate, and column temperature), the next seven are peak resolutions,  $Y_i$  ( $i=1, \dots, 7$ ) and the final vertical line is the coordinate of final time,  $t_f$  after undoing the transformation of  $Y_8$ . To avoid the different scales, the data have been scaled to a common range, and the original bounds have been written at the top and bottom of each coordinate, for reference. These bounds show that the found experimental conditions are in a restricted area: from 37 to 40 % of water, mixed with up to 22 % methanol, and less than 60 % of acetonitrile (in the corresponding proportions), linked to high values of flow rate (greater than  $1.39 \text{ mL min}^{-1}$ ) and temperatures greater than  $39.53 \text{ }^\circ\text{C}$ . The upper bounds of the last two factors are those already established for the experimental domain,  $1.50 \text{ mL min}^{-1}$  and  $44 \text{ }^\circ\text{C}$ . Besides the obvious relation among the mixture variables, the broken lines joining solutions in Fig. 2 should also be followed, no any condition in the ranges just stated can be used. For instance, if say  $Z_1 = 0.40$  (40 % of water) is chosen, then  $Z_2$  cannot be 0.22 (there is no line between 40 % of water and 22 % of methanol), or lower flow rates ( $X_4$ ) are linked to high temperatures ( $X_5$ ) with necessarily near 60 % of acetonitrile ( $Z_3$ ), and so on.

### 3.3. Determination of the MODR

The solutions in the Pareto front in Fig. 2 are a discrete version of the MODR, since their predicted values of CQA fulfil the established ATP, that is, all the peaks are expected to be well resolved, with final time less than 14 minutes, below the established limit. Therefore, their analysis and experimental validation can be seen as the robustness study of the chromatographic method, though in an approach different from the usual one.

In the proposed analysis, the 300 solutions in the Pareto front are the starting point. According to the PLS2 model fitted, they all fulfil the limits on the CQA but they should be experimentally validated.

As previously mentioned, when analyzing the solutions in Fig. 2, special attention must be paid to  $Y_4$  and, above all,  $Y_7$  which is the only one with several solutions near its lower constraint (the one imposed on the Pareto optimal solutions). In that situation,

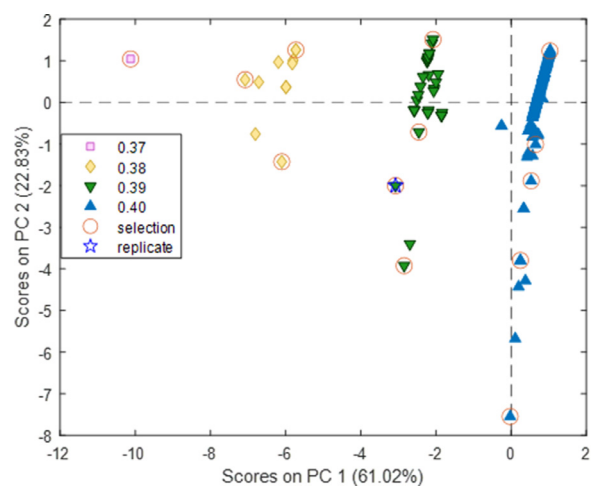


**Fig. 3.** Scores of the CMP in the Pareto front on the first plane of principal components. The colors vary with water content. The points selected for the experimental validation are surrounded by a circle; the star marks the experiment replicated four times.

the best (minimum) final time to achieve the desired resolutions is 12.12 minutes. However, there are more solutions in the Pareto front with more than 12.5 minutes and up to 14 minutes (the imposed upper constraint), with the resolutions farther from 1.5.

In this time range, extreme solutions are colored in Fig. 2: the orange dot dashed line points to a mobile phase with a binary mixture of water ( $Z_1$ , 0.40) and acetonitrile ( $Z_3$ , 0.60), a flow rate of  $1.5 \text{ mL min}^{-1}$  and  $39.53 \text{ }^\circ\text{C}$  to have all the resolutions greater than 1.53 (approximately) and a final time of 14 minutes. The other extreme, the continuous magenta line, says that the shortest chromatogram is expected when using a ternary mixture of around 0.39 of water ( $Z_1$ ), 0.06 of methanol ( $Z_2$ ), and 0.55 of acetonitrile ( $Z_3$ ), at the maximum flow rate and temperature,  $1.5 \text{ mL min}^{-1}$  and  $44 \text{ }^\circ\text{C}$ , respectively, but they will have 'limiting' values of resolution in  $Y_7$  and almost in  $Y_4$ .

In any case, all these characteristics describe chromatograms that are considered to be good enough for the determination (according to the predicted values of CQA), as difference of two minutes are not significant in the present context (above all comparing to the experiment that took 435 minutes to finish).

The question now is to experimentally validate the 'region' implicitly defined with these conditions, that is, to check that the expected characteristics of the chromatograms are indeed obtained when moving in the experimental domain. In practice, that means that chromatograms similar enough to be equally valid to conduct the determination are obtained.

Evidently, conducting the 300 experiments in Fig. 2 is not viable. To select some of them, representative of the whole set, a Principal Component Analysis (PCA) was done with the experimental conditions (the first five coordinates in Fig. 2), after autoscaling them.

Again with crossvalidation with venetian blinds (ten splits and blind thickness equal to one), two principal components are selected that explain 83.85 % of the variance in the 300 experimental conditions.

Fig. 3 shows the scores on the first plane (second versus first principal components) that form like a triangle, similar to a mixture's simplex. To explore this perception, scores have been colored and marked according to the amount of water: the pink square at the top left is the only solution with 37 % of water, yellow diamonds are for 38 % of water, green down triangles are for 39 % and blue up triangles for 40 % of water content. A similar schema would be seen if the scores were colored by methanol or acetonitrile.

**Table 3**  
Loadings on the first two principal components (PC).

Variable	Loading on PC1	Loading on PC2
Z <sub>1</sub> : water	0.5650	-0.0895
Z <sub>2</sub> : methanol	-0.5681	0.0935
Z <sub>3</sub> : acetonitrile	0.5669	-0.0940
X <sub>4</sub> : flow rate	0.0554	0.7643
X <sub>5</sub> : temperature	-0.1835	-0.6247

**Table 4**  
Experimental conditions for the experimental validation of the MODR.

Number	Z <sub>1</sub>	Z <sub>2</sub>	Z <sub>3</sub>	X <sub>4</sub>	X <sub>5</sub>
1	0.370	0.220	0.410	1.500	44.0
2	0.380	0.130	0.490	1.500	41.9
3	0.390	0.060	0.550	1.500	40.1
4	0.400	0.000	0.600	1.500	39.6
5	0.400	0.000	0.600	1.480	41.9
6	0.400	0.000	0.600	1.470	42.5
7	0.400	0.000	0.600	1.450	44.0
8	0.400	0.000	0.600	1.390	44.0
9	0.390	0.060	0.550	1.440	44.0
10	0.380	0.130	0.490	1.470	43.8
11	0.380	0.160	0.460	1.500	44.0
12	0.390	0.060	0.550	1.480	42.3
13*	0.390	0.070	0.540	1.470	44.0

\* This experiment is replicated four times.

trile content, as can be concluded from the loadings on the first principal component in Table 3. The loadings on the second principal component show the opposition between flow rate and temperature.

Accordingly, experimental conditions along the 'boundary' of the convex hull made up by the scores in Fig. 3 are selected, and circled in Fig. 3, with four replicates in the point marked with a star. That means that there are 16 experiments to be conducted to check the predictions. Their experimental conditions are collected in Table 4, where experiment number 13 is the one replicated to obtain an estimation of the experimental variation.

The results obtained with the CMP in Table 4 are summarized in Fig. 4 where the number in the abscissae axes identifies the experimental conditions according to the number in Table 4. Notice that there are only twelve because experiment number 13 was used exclusively to obtain an external estimate of the standard deviation.

Figs. 4A)-4H), separately for each response, show the experimental result in green together with its 95 % confidence interval, computed with the standard deviation obtained with the four replicates and a student *t* distribution with three degrees of freedom. The grey points and lines are the values predicted with the PLS2 model, and the corresponding confidence interval, computed by using the Root Mean Square Error in Prediction (RMSEP), also at 95 % confidence level.

As can be seen, every interval on the predicted responses, in grey, contain the experimentally obtained results (in fact the whole confidence interval in green), meaning that these experimental results are among those expected with the PLS2 model. On the contrary, only 27 out of 96 intervals computed with the experimental standard deviation (in green in Fig. 4) contain the predicted values (grey points).

It has already been said that responses Y<sub>4</sub> and Y<sub>7</sub>, resolutions R<sub>S67</sub> and R<sub>S89</sub>, are critical in the sense that their lower bounds in the 300 solutions of the Pareto front (Fig. 2) are very close to 1.5. Fig. 4D) for Y<sub>4</sub> shows that seven out of twelve experimental values (in green) are significantly greater than those estimated with the PLS2 prediction (their 95 % confidence intervals do not contain the predicted value), which is not the case for Y<sub>7</sub> (Fig. 4G)).

In Y<sub>7</sub>, only the experimental conditions in 1, 2, 10, and 11 provide acceptable values (resolutions 1.53, 1.47, 1.47, and 1.52, respectively) and significantly equal to the predicted ones, while the experimental conditions of the remaining eight experiments provide experimental values significantly less than the predicted ones. In detail, experimental conditions from experiment 4 to 8 have Y<sub>7</sub> = R<sub>S89</sub> around 1.2, which is too low with the ATP imposed to the chromatograms. Looking at Table 4, all of them are binary mixtures water/acetonitrile (40:60). Intermediates values of R<sub>S89</sub> are obtained in experiments 3, 9, and 12 though still unacceptable. All those cases have the same mixture in the mobile phase, 39:6:55 of water/methanol/acetonitrile with different flow rates and temperatures. Besides, except for experiments 1, 2, 10, and 11, the final time is less than the one estimated with PLS2 (Fig. 4H) at the expense of reducing the resolution between peaks 8 and 9 (Y<sub>7</sub>).

The scores in Fig. 3 of these experimental conditions (1, 11, 10, and 2) are the four circles on the left, namely with score in the first principal component less than -4. Therefore, the subsequent MODR occupies a smaller area (to the left of Fig. 3) than the region where the Pareto optimal solutions in Fig. 2 vary (seen as the whole representation in Fig. 3).

#### 3.4. Experimental validation of the MODR

The MODR sought is the convex envelope of the four conditions mentioned above. For the sole purpose of checking the validity (experimental validation) of the MODR, another 14 settings of the CMP have been selected that define experiments to be carried out in this region, those listed in Table 5, numbered from 14 to 27 to avoid confusion with the previous ones in Table 4. As can be seen, experiment number 24 is replicated three times.

The projection of these new experimental conditions on the plane in Fig. 3 is depicted in Fig. 5, red filled squares with the numbers in Table 5. The blue circles are the scores previously identified with the numbers in Table 4.

The experimental conditions in 16, 24, 17, and 18 in Fig. 5 and Table 5 are indeed the same as those in 1, 11, 10, and 2 of Table 4. The experiments numbered from 21 to 27 were obtained as convex combinations of these four. For example, the experimental conditions in experiment number 25, (Z<sub>1,25</sub>, Z<sub>2,25</sub>, Z<sub>3,25</sub>, X<sub>4,25</sub>, X<sub>5,25</sub>), are obtained as  $\lambda (Z_{1,2}, Z_{2,2}, Z_{3,2}, X_{4,2}, X_{5,2}) + (1 - \lambda)(Z_{1,10}, Z_{2,10}, Z_{3,10}, X_{4,10}, X_{5,10})$  with  $\lambda=0.5$  and it is at the boundary of the defined region in Fig. 5. Analogously, (Z<sub>1,21</sub>, Z<sub>2,21</sub>, Z<sub>3,21</sub>, X<sub>4,21</sub>, X<sub>5,21</sub>) is computed from (Z<sub>1,1</sub>, Z<sub>2,1</sub>, Z<sub>3,1</sub>, X<sub>4,1</sub>, X<sub>5,1</sub>) and (Z<sub>1,11</sub>, Z<sub>2,11</sub>, Z<sub>3,11</sub>, X<sub>4,11</sub>, X<sub>5,11</sub>) and it is already in the interior of the explored region. In this way, any point inside the convex envelope can be reached.

Finally, to deeply explore the combination of experimental conditions obtained, a grid on the CMPs is computed and projected onto the PCA plane. The combinations cover the selected region extending a little further than the exterior triangle in blue in Fig. 5, above all along the second principal component. Consequently, four additional conditions were selected at the vertices and at the middle of the uncommon edges. These are the experimental conditions 14, 15, 19, and 20 in Fig. 5 that define a polygon in red containing the triangle.

In that way, the entire MODR is covered and somehow slightly enlarged. The new experimental conditions and the properties of the corresponding chromatograms, in terms of the CQA (resolutions and final time), are in Table 5.

Regarding variable Y<sub>7</sub>, the values remain between 1.60 and 1.39, reaching these extreme values in conditions 19 and 20, respectively, placing this last one somehow near the boundary of the MODR. In any case, the results confirm the validity of the MODR obtained.

In conclusion, the estimated MODR is formed by the settings of the CMP in Table 5 and their convex combinations whose projec-

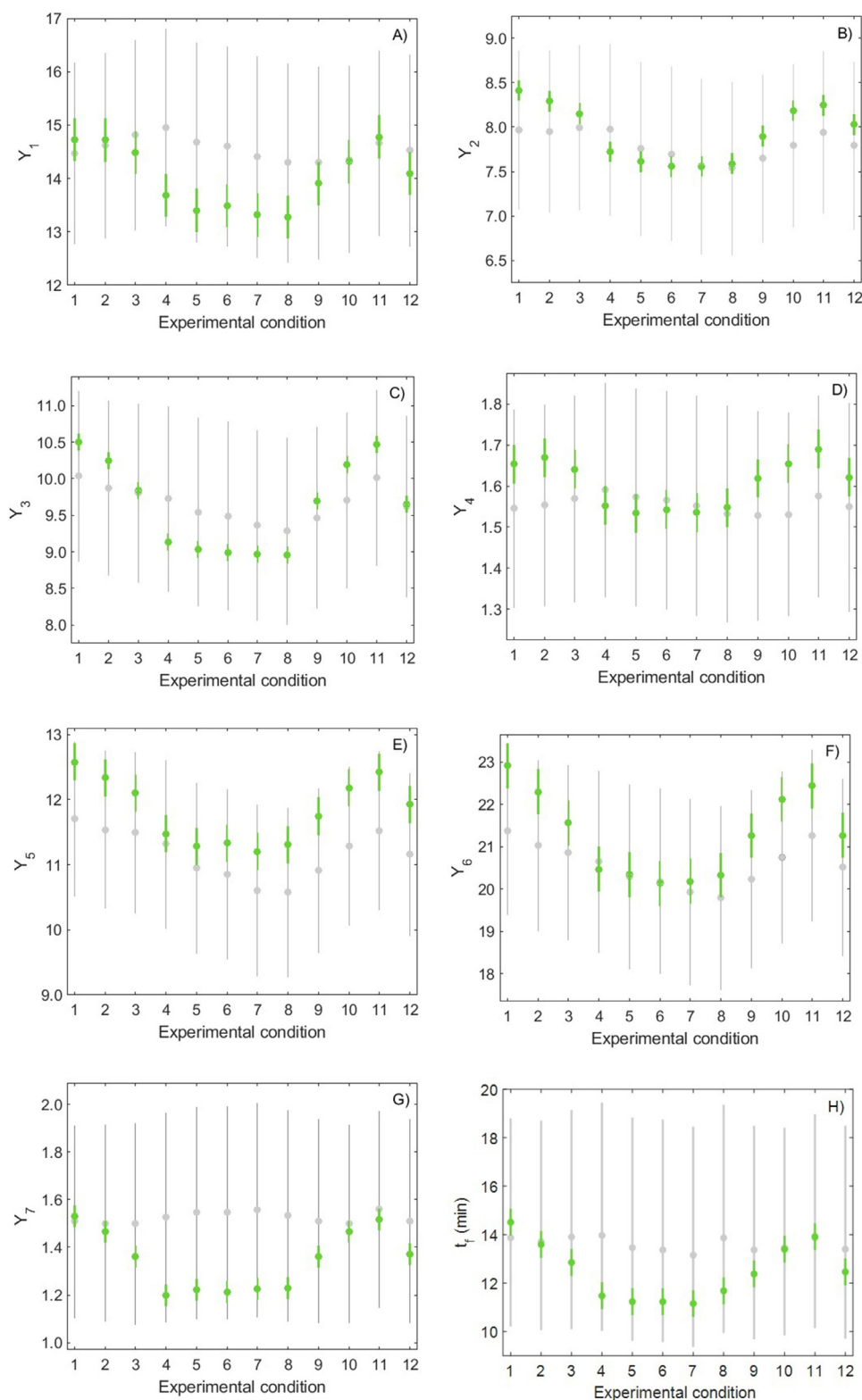


**Fig. 4.** Values and confidence intervals for the experimental conditions in Table 4 (in green) and for those predicted with the PLS2 model (in grey).

tion onto the PCA plane are inside the polygon in red in Fig. 5. As already said, Fig. 1C) depicts the chromatograms obtained in one of the conditions of this estimated MODR, specifically experiment number 19 in Table 5.

It is worth remembering that the experimental conditions in the MODR guarantee the validity of the chromatograms in the

terms established in the ATP. In particular, the method is robust while remaining in the MODR. However, the AQBd approach to establishing the MODR is the opposite of the classical procedure to verify the robustness of an analytical method. In the first case, the specifications on the CQA are first set and then the CMP values are obtained, precisely those settings with which the established

**Table 5**  
Experimental conditions and results for the experimental validation of MODR.

Number	Experimental conditions					Responses							
	Z <sub>1</sub>	Z <sub>2</sub>	Z <sub>3</sub>	X <sub>4</sub>	X <sub>5</sub>	Y <sub>1</sub>	Y <sub>2</sub>	Y <sub>3</sub>	Y <sub>4</sub>	Y <sub>5</sub>	Y <sub>6</sub>	Y <sub>7</sub>	t <sub>f</sub> (min)
14	0.370	0.220	0.410	1.500	42.0	15.16	8.62	10.85	1.72	12.87	23.10	1.54	15.154
15	0.370	0.220	0.410	1.470	44.0	14.58	8.36	10.60	1.68	12.73	22.63	1.51	14.661
16	0.370	0.220	0.410	1.500	44.0	14.58	8.37	10.54	1.68	12.70	22.65	1.52	14.389
17	0.380	0.130	0.490	1.470	43.8	14.26	8.06	10.04	1.66	12.02	22.01	1.43	13.119
18	0.380	0.130	0.490	1.500	41.9	14.43	8.26	10.20	1.66	12.36	22.07	1.45	13.448
19	0.380	0.190	0.430	1.500	42.0	15.44	8.67	10.83	1.73	12.81	23.29	1.60	15.657
20	0.370	0.160	0.470	1.470	44.0	14.18	8.16	10.08	1.63	12.21	21.66	1.39	12.964
21	0.375	0.190	0.435	1.500	44.0	14.58	8.33	10.50	1.68	12.47	22.38	1.53	14.116
22	0.374	0.184	0.442	1.500	43.2	14.65	8.30	10.42	1.68	12.53	22.38	1.49	14.102
23	0.376	0.166	0.458	1.482	43.9	14.47	8.28	10.25	1.64	12.29	22.33	1.48	13.689
24	0.380	0.160	0.460	1.500	44.0	14.61	8.35	10.45	1.70	12.40	22.34	1.51	13.860
24	0.380	0.160	0.460	1.500	44.0	14.57	8.29	10.38	1.68	12.37	22.49	1.52	13.947
24	0.380	0.160	0.460	1.500	44.0	14.61	8.29	10.39	1.66	12.28	22.18	1.51	13.931
25	0.380	0.130	0.490	1.485	42.9	14.53	8.18	10.08	1.64	12.24	22.06	1.44	13.358
26	0.380	0.145	0.475	1.500	43.0	14.17	8.15	10.17	1.66	12.44	21.99	1.44	13.460
27	0.380	0.142	0.478	1.482	43.9	14.27	8.08	10.07	1.64	12.20	21.80	1.45	13.307

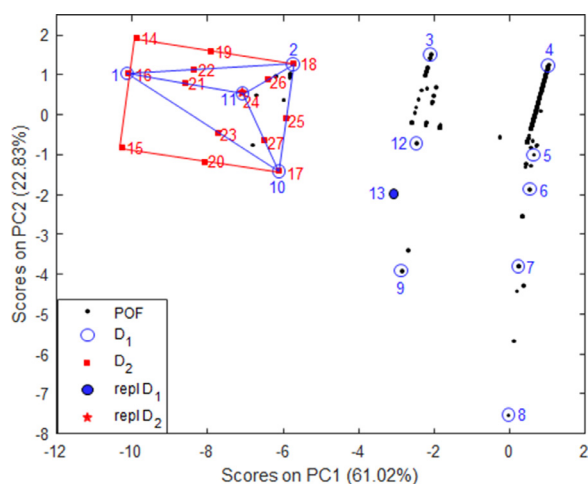


**Fig. 5.** Scores of CMP on the PCA plane. Experiments identified with the numbers in Table 4 and Table 5, surrounded by a blue circumference, and red filled squares, respectively. Filled blue circle and red star are the replicated experiments.

quality of the chromatograms is maintained. In this sense, the obtained information is on how the CMP should vary to maintain adequate values of CQA.

On the contrary, the conventional way to determine robustness needs to previously set the values for all CPM and, then, vary each by a *reasonable* amount so that the obtained CQA values can be considered "equal". To decide whether the variation caused in the CQA values by the change in the CPM is significantly null or not, a screening design (Plackett Burman, fractional, etc.) is usually used.

Furthermore, it is not only that the procedure to establish robustness starts from the CQA or the CMP depending on the approach, but also the fact that, in computing the MODR, the robustness is built taking into account the internal relations of the CMP, the CQA, and between one another. This implies that inside the MODR obtained, once the value of one of the CPM has been set, the others must maintain the appropriate relation, in the present case, the same convex combination with those in Table 5. In the classical approach, on the contrary, it is assumed that there is no relation among CMP, because with screening designs the interactions are confounded with the main effects (i.e., the effect of the change in CMP on CQA).

### 3.5. Comparative performance and figures of merit of the analytical method

The performance of the analytical procedure in the estimated MODR is better than other procedures found in the literature: from the several documents returned in a bibliographic search with "polycyclic aromatic hydrocarbon AND HPLC AND fluorescence" in 2019-2021, only those where the published chromatographic determinations include at least two of the compounds considered here were selected. Table S1 in the supplementary material shows a comparison of the results shown in the present paper and those obtained in 28 of such published papers.

Columns 3 to 5 of Table S1 show the experimental factors in relation to the ones used in the present paper: mixture and flow rate of mobile phase and column temperature. Most of the papers (25 of 28) report the use of binary mixtures of acetonitrile/water, in which gradient elution mode has been carried out except for three papers. In these three, gradient elution mode is used but with a binary mixture of methanol/water, and two ternary mixtures of acetonitrile/tetrahydrofuran/water and acetonitrile/methanol/water. Several different values were reported for flow rate and temperature, between 0.25 and 2.20 mL min<sup>-1</sup>, and 20 and 40 °C, respectively. In the present work, the MODR includes working with 1.5 mL min<sup>-1</sup> and 44 °C, and by using ternary mixtures (water/methanol/acetonitrile) in the corresponding proportion indicated in Table 5.

Column 6 of Table S1 in the supplementary material summarizes the number of PAHs analyzed in the mentioned papers, out of the 10 PAHs determined in the present work. The table also contains the retention time of the BaP, which is the compound that elutes in tenth position. Comparing to the final time in the established MODR, eight papers show less retention time of BaP, though only 3 or 4 PAHs were determined in five of them. The other three papers, in which 8 or 9 PAHs were analyzed, have chromatograms that show several overlapping peaks or peaks with very bad resolution.

In order to compute the figures of merit of the analytical method, the experimental conditions corresponding to experiment number 19 in Table 5 (related to the chromatogram in Fig. 1C), are used.

The analytical procedure is validated in terms of linear range, accuracy (trueness and precision), decision limit (CC $\alpha$ ) and detection capability (CC $\beta$ ) for the ten PAHs under study. CC $\alpha$  and CC $\beta$  are determined with probabilities of false positive ( $\alpha$ ) and false negative ( $\beta$ ) set at 0.05, following Refs. [26,27]. Table 6 contains

**Table 6**  
Retention times, characteristics of calibration lines (in the overall range and around the detection limit) and accuracy lines (in the overall range), decision limit,  $CC\alpha$ , and detection capability,  $CC\beta$ , with  $\alpha = \beta = 0.05$  ( $n = 6$ ,  $r = 2$ ),  $s_{yx}$  is the standard error of the estimate.

#	NAP	PHE	ANT	FLN	PYR	CHR	BaA	PER	BbF	BaP
1	2.758 ± 0.009	4.818 ± 0.012	5.225 ± 0.013	6.446 ± 0.014	6.891 ± 0.013	9.652 ± 0.017	10.170 ± 0.018	13.390 ± 0.020	14.038 ± 0.023	14.971 ± 0.023
2	0 - 500	0 - 500	0 - 2000	0 - 300	0 - 150	0 - 100	0 - 40	0 - 200	0 - 150	0 - 30
3	-0.052	-0.115	0.066	-0.077	-0.643	-0.211	-0.835	-0.130	-0.180	-0.573
4	0.142	0.130	0.025	0.154	0.810	0.352	1.105	1.637	0.311	1.637
5	<10 <sup>-4</sup>	<10 <sup>-4</sup>	<10 <sup>-4</sup>	<10 <sup>-4</sup>	<10 <sup>-4</sup>	<10 <sup>-4</sup>	<10 <sup>-4</sup>	<10 <sup>-4</sup>	<10 <sup>-4</sup>	<10 <sup>-4</sup>
6	0.9999	0.9999	0.9999	1.0000	0.9996	0.9998	0.9998	0.9999	0.9998	0.9988
7	0.331	0.218	0.189	0.116	1.074	0.220	0.676	0.192	0.326	0.764
8	0	0	0	1	0	0	0	1	0	0
9	6.98 10 <sup>-10</sup>	-1.82 10 <sup>-6</sup>	-9.22 10 <sup>-7</sup>	5.95 10 <sup>-8</sup>	-1.91 10 <sup>-7</sup>	-7.52 10 <sup>-8</sup>	3.17 10 <sup>-7</sup>	-6.69 10 <sup>-7</sup>	8.06 10 <sup>-7</sup>	4.91 10 <sup>-8</sup>
10	0.999	1.000	0.999	0.999	1.000	1.000	0.999	1.000	0.999	1.000
11	2.339	1.683	7.524	0.756	1.326	0.626	1.058	1.047	1.047	0.467
12	1.000	1.000	1.000	1.000	1.000	1.000	1.000	1.000	1.000	1.000
13	0 - 40	0 - 40	0 - 300	0 - 40	0 - 20	0 - 20	0 - 12.5	0 - 40	0 - 20	0 - 10
14	-0.152	-0.159	0.053	-0.063	-0.130	-0.023	-0.274	-0.064	0.153	0.255
15	0.148	0.130	0.025	0.151	0.702	0.334	1.037	0.177	0.275	1.496
16	<10 <sup>-4</sup>	<10 <sup>-4</sup>	<10 <sup>-4</sup>	<10 <sup>-4</sup>	<10 <sup>-4</sup>	<10 <sup>-4</sup>	<10 <sup>-4</sup>	<10 <sup>-4</sup>	<10 <sup>-4</sup>	<10 <sup>-4</sup>
17	0.9973	0.9927	0.9998	0.9996	0.9916	0.9970	0.9981	0.9990	0.9964	0.9946
18	0.163	0.239	0.060	0.067	0.707	0.198	0.298	0.121	0.181	0.585
19	1.6	2.7	3.6	0.6	1.5	0.9	0.5	1.0	1.0	0.6
20	3.2	5.3	7.0	1.3	3.0	1.8	0.9	2.0	2.0	1.2
	<b>Calibration line (overall range)</b>									
	Linear range ( $\mu\text{g L}^{-1}$ )									
	Intercept									
	Slope									
	P-value ( $H_0$ : Model is not significant)									
	Correlation coefficient									
	$s_{yx}$									
	Number of outliers									
	<b>Accuracy line (overall range)</b>									
	Intercept									
	Slope									
	$s_{yx}$									
	P-value ( $H_0$ : Intercept = 0 and slope = 1)									
	<b>Calibration line (detection limit)</b>									
	Linear range ( $\mu\text{g L}^{-1}$ )									
	Intercept									
	Slope									
	P-value ( $H_0$ : Model is not significant)									
	Correlation coefficient									
	$s_{yx}$									
	$CC\alpha$ ( $\mu\text{g L}^{-1}$ )									
	$CC\beta$ ( $\mu\text{g L}^{-1}$ )									

the corresponding retention times, the details of calibration and accuracy lines, and  $CC\alpha$  and  $CC\beta$  for the ten PAHs.

Calibration lines are fitted (one for each PAH) with the twelve standard solutions whose range is showed in row number 2 in Table 6 (all concentration levels are replicated twice). Rows number 3 to 8 in Table 6 show the parameters of the regression lines, which are all statistically significant because the  $P$ -values (row 5) of the significance test are less than  $10^{-4}$  (null hypothesis  $H_0$ : the regression model is not significant).

Trueness and precision are checked using accuracy lines (that is, predicted concentration vs true concentration). Their details are in rows 9 to 12 of Table 6, including the  $P$ -values of the joint hypothesis test ( $H_0$ : intercept equal to zero and slope equal to one) in row 12. As can be observed, there is no evidence to reject  $H_0$  since the  $P$ -values are all 1, therefore, the method is unbiased. The precision of the method can be estimated by the standard errors,  $s_{yx}$  in row 11.

To compute decision limit ( $CC\alpha$ ) and detection capability ( $CC\beta$ ), new calibration lines are fitted with only the first six standards, with the range in row 13 of Table 6. These new calibration lines are also significant, according to the  $P$ -values in row 16 of Table 6, and provide the values of  $CC\alpha$  and  $CC\beta$  in rows 19 and 20 where it is seen that the analytical method enabled the quantification of 3.2, 5.3, 7.0, 1.3, 3.0, 1.8, 0.9, 2.0, 2.0, and 1.2  $\mu\text{g L}^{-1}$  for NAP, PHE, ANT, FLN, PYR, CHR, BaA, PER, BbF, and BaP, respectively.

#### 4. Conclusions

The Method Operable Design Region, MODR, of the chromatographic determination of ten PAHs by HPLC-FLD has been computed by using a PLS2 model that relates the CMP (experimental factors) and the CQA (responses). The inversion of this PLS2 model to find the Pareto front of optimal solutions is the key for starting the procedure.

The established MODR explicitly preserves the correlation among both the CMP and the CQA by considering convex combinations of the chromatographic conditions that form the MODR. In particular, the MODR includes robust experimental conditions for the determination of ten PAHs with well resolved peaks and final time around 15 minutes.

The joint representation, by means of a parallel coordinate plot, of CMP settings and the corresponding values of CQA in the Pareto front allows the MODR to be displayed in a single graph, therefore avoiding the need of keeping constant some of the CMP to be able to obtain "overlapping maps" of the ATP specifications on CQA with the subsequent risk of misinterpretation. This is increasingly important as the number of specifications considered in the ATP grows.

The experimental validation of the MODR avoids the arbitrary assignment of probability distributions to the CMP and their propagation to the CQA.

The proposed methodology is general and can be used for other types of chromatographic separations, or even for other instrumental applications.

#### Declaration of Competing Interest

The authors declare that they have no known competing financial interests or personal relationships that could have appeared to influence the work reported in this paper.

#### CRediT authorship contribution statement

**M.M. Arce:** Investigation, Methodology, Writing – original draft, Writing – review & editing. **S. Sanllorente:** Investigation, Supervision, Writing – review & editing. **S. Ruiz:** Formal analysis, Method-

ology, Writing – review & editing. **M.S. Sánchez:** Conceptualization, Formal analysis, Funding acquisition, Methodology, Supervision, Writing – review & editing. **L.A. Sarabia:** Conceptualization, Formal analysis, Methodology, Software, Supervision, Writing – original draft, Writing – review & editing. **M.C. Ortiz:** Conceptualization, Formal analysis, Methodology, Software, Supervision, Writing – original draft, Writing – review & editing.

## Acknowledgments

The work is part of research projects CTQ2017-88894-R and BU052P20, financed by the Spanish Ministerio de Ciencia, Innovación y Universidades (AEI/FEDER, UE) and Consejería de Educación de la Junta de Castilla y León, both co-financed with European Development Funds. M.M. Arce wishes to thank Junta de Castilla y León for her postdoctoral contract through BU052P20 project.

## Supplementary materials

Supplementary material associated with this article can be found, in the online version, at doi:[10.1016/j.chroma.2021.462577](https://doi.org/10.1016/j.chroma.2021.462577).

## References

- [1] Food and Drug AdministrationPAT - A Framework for Innovative Pharmaceutical Development, Manufacturing and Quality Assurance, Guidance for Industry, Pharmaceutical CGMPs, Rockville, September 2004 <https://www.fda.gov/media/71012/download>.
- [2] European Medicines AgencyInternational Conference on Harmonisation of Technical Requirements for Registration of Pharmaceuticals for Human Use considerations (ICH) guideline Q8 (R2) on pharmaceutical development - Step 5, June 2017 <https://www.ema.europa.eu/en/ich-q8-r2-pharmaceutical-development> (accessed 5 July 2021).
- [3] E. Rozet, P. Lebrun, P. Hubert, B. Debrus, B. Boulanger, Design spaces for analytical methods, TRAC-Trend. Anal. Chem. 42 (2013) 157–167, doi:[10.1016/j.trac.2012.09.007](https://doi.org/10.1016/j.trac.2012.09.007).
- [4] R. Peraman, J. Bandi, V.K. Kondreddy, B. Kalva, S.G. Kothakota, J. Paritala, K. Nagappan, P.R. Yirgamreddy, Analytical quality by design approach versus conventional approach: Development of HPLC-DAD method for simultaneous determination of etizolam and propranolol hydrochloride, J. Liq. Chromatogr. R. T. 44 (3–4) (2021) 197–209, doi:[10.1080/10826076.2021.1874982](https://doi.org/10.1080/10826076.2021.1874982).
- [5] R. Deidda, S. Orlandini, P. Hubert, C. Hubert, Risk-based approach for method development in pharmaceutical quality control context: a critical review, J. Pharmaceut. Biomed 161 (2018) 110–121, doi:[10.1016/j.jpba.2018.07.050](https://doi.org/10.1016/j.jpba.2018.07.050).
- [6] T. Tome, N. Žigart, Z. Časar, A. Obreza, Development and Optimization of Liquid Chromatography Analytical Methods by Using AQbD Principles: Overview and Recent Advances, Org. Process Res. Dev. 23 (9) (2019) 1784–1802, doi:[10.1021/acs.oprd.9b00238](https://doi.org/10.1021/acs.oprd.9b00238).
- [7] R. Peraman, K. Bhadrara, Y.P. Reddy, Analytical Quality by design: a tool for regulatory flexibility and robust analytics, Int. J. Anal. Chem. 868727 (2015) 1–9, doi:[10.1155/2015/868727](https://doi.org/10.1155/2015/868727).
- [8] P. Lebrun, B. Boulanger, B. Debrus, P. Lambert, P. Hubert, A Bayesian design space for analytical methods based on multivariate models and predictions, J. Biopharm. Stat. 23 (6) (2013) 1330–1351, doi:[10.1080/10543406.2013.834922](https://doi.org/10.1080/10543406.2013.834922).
- [9] S. Orlandini, B. Pasquini, C. Caprini, M. Del Bubba, L. Squarzialupi, V. Colotta, S. Furlanetto, A comprehensive strategy in the development of a cyclodextrin-modified microemulsion electrokinetic chromatographic method for the assay of diclofenac and its impurities: mixture-process variable experiments and quality by design, J. Chromatogr. A 1466 (2016) 189–198, doi:[10.1016/j.chroma.2016.09.013](https://doi.org/10.1016/j.chroma.2016.09.013).
- [10] M.C. Ortiz, L.A. Sarabia, A. Herrero, C. Reguera, S. Sanlloriente, M.M. Arce, O. Valencia, S. Ruiz, M.S. Sánchez, Partial Least Squares model inversion in the chromatographic determination of triazines in water, Microchem. J. 164 (2021) 105971, doi:[10.1016/j.microc.2021.105971](https://doi.org/10.1016/j.microc.2021.105971).
- [11] M.M. Arce, S. Ruiz, S. Sanlloriente, M.C. Ortiz, L.A. Sarabia, M.S. Sánchez, A new approach based on inversion of a partial least squares model searching for a preset analytical target profile. Application to the determination of five bisphenols by liquid chromatography with diode array detector, Anal. Chim. Acta 1149 (2021) 338217, doi:[10.1016/j.aca.2021.338217](https://doi.org/10.1016/j.aca.2021.338217).
- [12] S. Ruiz, M.C. Ortiz, L.A. Sarabia, M.S. Sánchez, A computational approach to partial least squares model inversion in the framework of the process analytical technology and quality by design initiatives, Chemometr. Intell. Lab. 182 (2018) 70–78, doi:[10.1016/j.chemolab.2018.08.014](https://doi.org/10.1016/j.chemolab.2018.08.014).
- [13] J.P. Longwell, The formation of polycyclic aromatic hydrocarbons by combustion, Symposium (International) on Combustion 19 (1) (1982) 1339–1350, doi:[10.1016/S0082-0784\(82\)80310-X](https://doi.org/10.1016/S0082-0784(82)80310-X).
- [14] United States Environmental Protection Agency, Toxic and Priority Pollutants Under the Clean Water Act. <https://www.epa.gov/eg/toxic-and-priority-pollutants-under-clean-water-act> (accessed 14 July 2021).
- [15] International Agency for Research on CancerIARC monographs on the identification of carcinogenic hazards to humans, World Health Organization, 2019 <https://monographs.iarc.who.int/list-of-classifications> (accessed 15 July 2021).
- [16] Commission regulation (EU) No. 1881/2006 of 19 December 2006 setting maximum levels for certain contaminants in foodstuffs, Off. J. Eur. Union L 364 (2006) 5–24.
- [17] Commission Regulation (EU) No 835/2011 of 19 August 2011 amending Regulation (EC) No 1881/2006 as regards maximum levels for polycyclic aromatic hydrocarbons in foodstuffs, Off. J. Eur. Union L 215 (2011) 4–8.
- [18] B.M. Wise, N.B. Gallagher, R. Bro, J.M. Shaver, W. Winding, R.S. Koch, PLS Toolbox 8.8.1, Eigenvector Research Inc., Wenatchee, WA, USA, 2020.
- [19] MATLAB, version 9.7.0.1190202 (R2019b), The Mathworks, Inc., Natick, MA, USA, 2019.
- [20] D. Mathieu, J. Nony, R. Phan-Thau-Lu, NEMRODW (Version 2015), L.P.R.A.I., Marseille, France, 2015.
- [21] L.A. Sarabia, M.C. Ortiz, M.S. Sánchez, Response surface methodology, in: S. Brown, R. Tauler, B. Walczak (Eds.), Comprehensive Chemometrics. Chemical and Biochemical Data Analysis, second ed., Elsevier, 2020, pp. 287–326, doi:[10.1016/B978-0-12-409547-2.14756-0](https://doi.org/10.1016/B978-0-12-409547-2.14756-0).
- [22] C.M. Jaeckle, J.F. MacGregor, Industrial applications of product design through the inversion of latent variable models, Chemometr. Intell. Lab. 50 (2) (2000) 199–210, doi:[10.1016/S0169-7439\(99\)00058-1](https://doi.org/10.1016/S0169-7439(99)00058-1).
- [23] D. Palací-López, P. Villalba, P. Facco, M. Barolo, A. Ferrer, Improved formulation of the latent variable model inversion-based optimization problem for quality by design applications, J. Chemometr. 34 (2020) e3230, doi:[10.1002/cem.3230](https://doi.org/10.1002/cem.3230).
- [24] S. Ruiz, L.A. Sarabia, M.C. Ortiz, M.S. Sánchez, Residual spaces in latent variables model inversion and their impact in the design space for given quality characteristics, Chemometr. Intell. Lab. 203 (2020) 104040, doi:[10.1016/j.chemolab.2020.104040](https://doi.org/10.1016/j.chemolab.2020.104040).
- [25] P.F. Vanbel, P.J. Schoenmakers, Selection of adequate optimization criteria in chromatographic separations, Anal. Bioanal. Chem. 394 (2009) 1283–1289, doi:[10.1007/s00216-009-2709-9](https://doi.org/10.1007/s00216-009-2709-9).
- [26] International Organization for Standardization, ISO 11843, Capability of Detection, Part 1: Terms and Definitions and Part2: Methodology in the Linear Calibration Case, Genève, Switzerland, 2000.
- [27] Commission Decision (EC), No 2002/657/EC of 12 August 2002 Implementing Council Directive 96/23/EC Concerning the Performance of Analytical Methods and the Interpretation of Results, Off. J. Eur. Commun. L 221 (2002) 8–36.